Structure and properties of poly(tetrahydrofuran) viologen ionene: effects of halide counter-anions*

Tamotsu Hashimoto†, Shinichi Sakurai†‡, Masato Morimoto‡, Shunji Nomura‡, Shinzo Kohjiya§ and Toshiyuki Kodaira

Department of Materials Science and Engineering, Faculty of Engineering, Fukui University, Bunkyo, Fukui 910, Japan, ‡Department of Polymer Science and Engineering, Kyoto Institute of Technology, Matsugasaki, Sakyo-ku, Kyoto 606, Japan and §Institute for Chemical Research, Kyoto University, Uji, Kyoto 611, Japan

(Received 27 October 1993; revised 26 November 1993)

The effects of counter-anions on the microphase-separated structure and the properties of elastomeric ionene polymers (PTV) containing poly(tetrahydrofuran) (poly(THF)) soft-segment blocks and viologen hard ionic segments were investigated by thermal and mechanical analyses and by a small-angle X-ray scattering (SAXS) technique. Three sorts of PTVs having Cl^-, Br^-, or I^- halide ions as counter-anions for the viologen groups were synthesized. All PTVs showed good elastomeric properties, i.e. low tensile modulus, high tensile strength and high elongation at break. The PTV with Cl^- anions showed a higher capability of crystallization of the poly(THF) block chains than those with Br^- or I^- anions, in the cooling process prior to successive thermal and dynamic viscoelastic measurements, and exhibited a higher glass transition temperature of the amorphous poly(THF) chains in the heating process of these measurements. In the SAXS experiments, all PTVs exhibited multiple scattering peaks, indicating that microphase separation between the poly(THF) block chains and the viologen units was highly ordered. On the basis of these results, we considered a lamellar-type microphase-separated structure for PTVs with halide counter-anions.

(Keywords: poly(THF) viologen ionene; microphase-separated structure; thermal/mechanical properties)

INTRODUCTION

Elastomeric ionene is, in general, a multiblock-type linear polymer containing flexible polymeric segments and quaternary ammonium salts in the main chain, and can be classified as a sort of ionomer. We have already developed an elastomeric ionene polymer (abbreviated as PTV) consisting of poly(tetrahydrofuran) (or poly(oxytetramethylene)) (poly(THF)) segments and viologen groups[2-4]. As is often observed for other elastomeric ionenes[5-7], PTVs display high tensile strength and high elongation at break. Furthermore, PTVs were found to exhibit photo-induced properties such as photochromism[2,3] and a photomechanical effect[3] via photo-induced reaction of the viologen groups embedded in the PTV backbone.

The elastic nature of ionene polymers is considered to arise from ionic clustering: the electrostatic interaction of the quaternary ammonium ions through counter-anions leads to ionic aggregation in the flexible polymer matrix, and hence forms ion clusters, which behave like crosslinking points in vulcanized rubbers or hard-segment domains in polyurethanes. Thus, the role of the counter-anions should be very important, and the sort of counter-anion may influence the structure and properties of elastomeric ionenes. However, the effects of counter-anions have been studied for only a few ionenes[7-10].

In the present study, three kinds of PTVs with Cl^-, Br^-, or I^- counter-anions were prepared and their mechanical and thermal properties were investigated. Particular attention was focused on the microphase-separated structure of PTVs with halide counter-anions, since lamellar-type aggregation of the viologen groups was suggested by the results of small-angle X-ray scattering (SAXS).

EXPERIMENTAL

Synthesis of PTV

Figure 1 illustrates the synthesis route of PTVs with halide counter-anions[2]. Commercial tetrahydrofuran (THF) was dehydrated by calcium chloride overnight and refluxed and distilled twice over lithium aluminium hydride. Cationic bulk polymerization of THF (200 g) was conducted with trifluoromethanesulfonic anhydride ($(CF_3SO_2)_2O$; 5.03 g) at 0°C under dry nitrogen for 15 min ($[[(CF_3SO_2)_2O]_0 = 0.078\ mol\ l^{-1}$)[11]. The chain-extension

* This study was presented in part at a recent symposium[1]

† To whom correspondence should be addressed

0032-3861/94/12/2672-07

reaction of the bifunctional living polymer formed was carried out with an equimolar quantity of 4,4'-bipyridine (2.78 g) at 0°C for 90 min. The resulting viscous reaction mixture involving ionene-type polymer with sulfonate counter-anions was diluted with methanol (1.3 litre) and the diluted solution was divided into three portions (ca. 500 ml). Each portion was poured into aqueous solutions of 1.5 litre 10 wt% sodium chloride, sodium bromide or sodium iodide with vigorous stirring at room temperature. The precipitated polymers (PTV) having Cl^-, Br^-, or I^- as counter-anions were washed with deionized water and dried in a vacuum oven at 40°C; conversion of THF was ca. 20%. The quantitative exchanges of counter-anions were confirmed by elemental analysis of halogen (Cl, Br, or I) of the PTVs obtained.

Figure 2 shows the 270 MHz ^1H n.m.r. spectrum of PTV with Cl^- anions in CD_3OD at 30°C, along with peak assignments. Absorptions of two methylene groups of the poly(THF) chains (a and b) and pyridinium rings (e and f) are observed, and peaks c and d are assignable to the two methylenes adjacent to the pyridinium nitrogen. Signals indicative of side reactions are absent. On the basis of the peak intensity ratio of the methylene of the poly(THF) chains (peak a) and the viologen group (peaks e and f), the average molecular weight of the poly(THF) block chain of PTV was determined to be 1800.

Film specimens were prepared by casting ca. 3 wt% PTV solutions in methanol at 25°C for about 1 week and vacuum drying at 40°C for at least 3 days.

Measurements

Tensile stress–strain curves were obtained with a Shinkoh TOM-200D tensile tester at a crosshead speed of 10 mm min^{-1} at room temperature. Ring-shaped specimens (11.6 and 13.6 mm inner and outer diameters, respectively, and ca. 0.5 mm thickness) were subjected to measurement.

Differential scanning calorimetry (d.s.c.) was conducted with a MAC Science DSC 3100. The temperature range was −150 to +200°C and the heating rate was 5°C min^{-1}. During the experiment, the sample was purged by nitrogen gas.

Dynamic viscoelastic properties were measured with a Rheology Rheospectoler DVE-V4 in the temperature range −150 to +150°C. A synthesized wave comprising eight strain frequencies of 2^n Hz, where n is integer ($n=0$–7), was used for the measurement under a constant-temperature scan at a heating rate of 30°C min^{-1}. In this paper, only temperature dispersion at 128 Hz is presented.

Wide-angle X-ray diffraction (WAXD) patterns were taken with a Shimadzu GX3, operated at 40 kV and 20 mA. Film specimens at given stretching ratios were exposed to Cu Kα radiation for ca. 4 h and the diffracted X-rays recorded on flat photographic film. The sample-to-detector distance was 33.7 mm.

In order to get a sufficiently high signal-to-noise ratio from thin-film specimens of PTV, SAXS experiments were conducted using synchrotron radiation as the X-ray source at the BL-10C beamline in the Photon Factory of the National Laboratory for High Energy Physics, Japan. The incident beam was focused with a bent cylindrical mirror and monochromatized with a pair of Si(1 1 1) crystals. The wavelength λ of the incident beam was 0.1488 nm. The scattered intensity was detected at room temperature with a one-dimensional position-sensitive proportional counter. The sample-to-detector distance was 1.9 m. The details of the apparatus were described elsewhere[12]. The film normal is parallel to the propagation direction of the incident beam (through view). The observed SAXS data were corrected for air scattering and absorption due to the specimen. The data were further corrected for thermal diffuse scattering arising from density fluctuations.

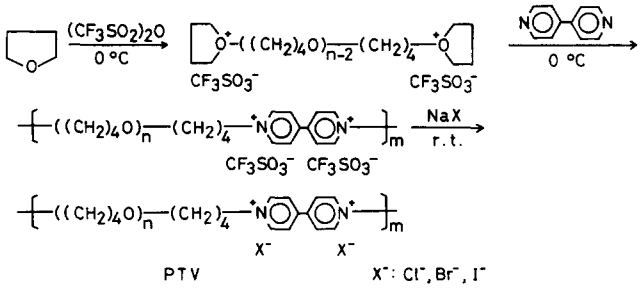

Figure 1 Synthesis route for PTVs with various halide counter-anions

RESULTS AND DISCUSSION

Tensile stress–strain properties

Figure 3 shows the tensile stress–strain behaviour of PTVs with three kinds of halide counter-anions, Cl^-,

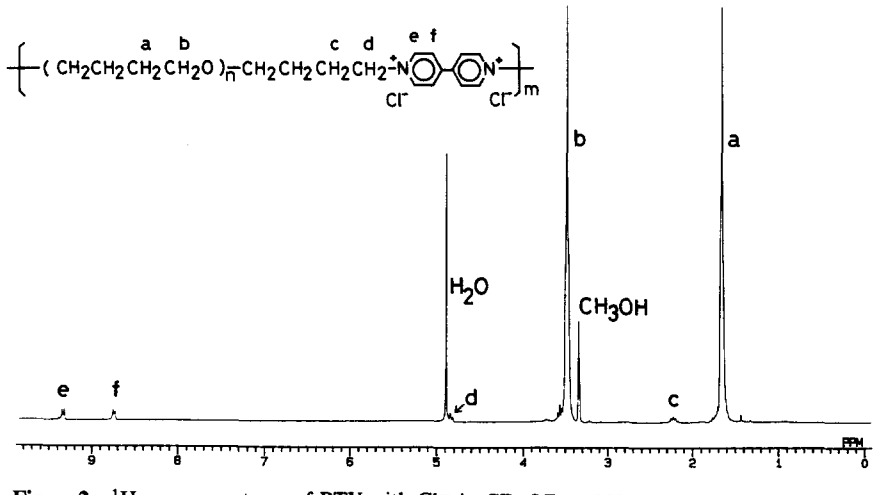

Figure 2 ^1H n.m.r. spectrum of PTV with Cl^- in CD_3OD at 30°C

Br^- and I^-. Note that the stress shown here is the nominal stress. As already reported for PTV with bromide anions[2–4], PTVs show elastomeric properties of high tensile strength and high elongation at break. Their tensile moduli were relatively low before 300% strain, but increased gradually with further elongation up to break.

WAXD measurements were conducted so as to elucidate the strain-induced crystallization, which can result in the drastic increase of stress after 300% strain, as shown in *Figure 3*. The observed patterns are presented for uniaxially stretched specimens of PTV with Br^- at 200%, 500% and 600% strains in *Figures 4a*, *4b* and *4c*, respectively. For 200% strain, only the amorphous halo was observed at a scattering angle of 19.6°, except for several scattering rings at 25.4°, 29.7° and 43.1°, which may be ascribed to diffraction from the crystals of viologen units. On the other hand, the (020) and (110) reflections[13] of the crystals of poly(THF) soft segments are clearly seen at 19.9° and 24.0° on the equator, and another weak (130) reflection is also observed at 37.6° on the equator for 500% strain. As for 600% strain, additional reflections from the poly(THF) crystals can definitely be detected at the off-equatorial positions 40.6° and 43.0°. Thus, the strain-induced crystallization of the poly(THF) chains is confirmed by the WAXD measurements, and hence the drastic increase of the stress can be attributed to crystallization of the poly(THF) chains of PTV. Similar strain-induced crystallization behaviour was observed for other poly(THF)-based ionenes with different ionic hard segments[14].

Thermal properties

Figure 5 shows d.s.c. thermograms of PTVs with Cl^-, Br^-, or I^- counter-anions in a heating process at a rate of 5°C min^{-1}. In this experiment, PTV specimens were first cooled to −180°C from room temperature at a cooling rate of ca. 20°C min^{-1} before successive d.s.c. measurements. During this cooling process, the poly(THF) soft segments of PTVs crystallized. Thus, in the heating process, all the PTV samples exhibited melting of the crystalline poly(THF) chains in the range of about −30 to +20°C. The glass transitions of the poly(THF) units were also detectable around −80°C on magnification of the thermograms, and are indicated with arrows in *Figure 5*. The broad peaks around 100°C may be due to slight moisture in the samples.

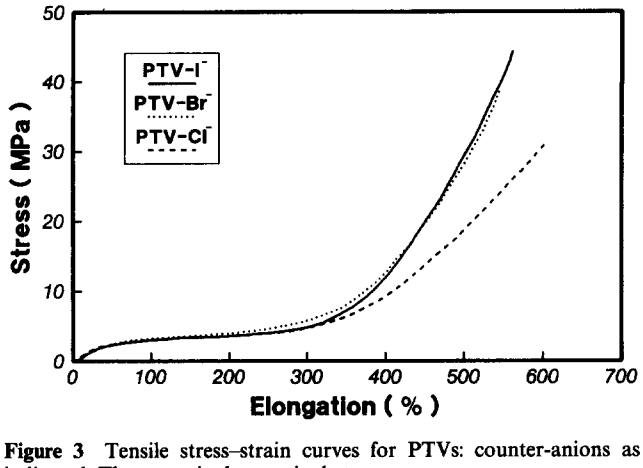

Figure 3 Tensile stress–strain curves for PTVs: counter-anions as indicated. The stress is the nominal stress

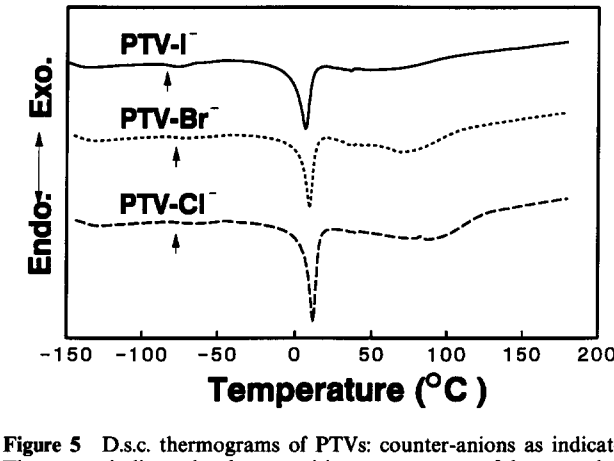

Figure 5 D.s.c. thermograms of PTVs: counter-anions as indicated. The arrows indicate the glass transition temperatures of the amorphous poly(THF) chains

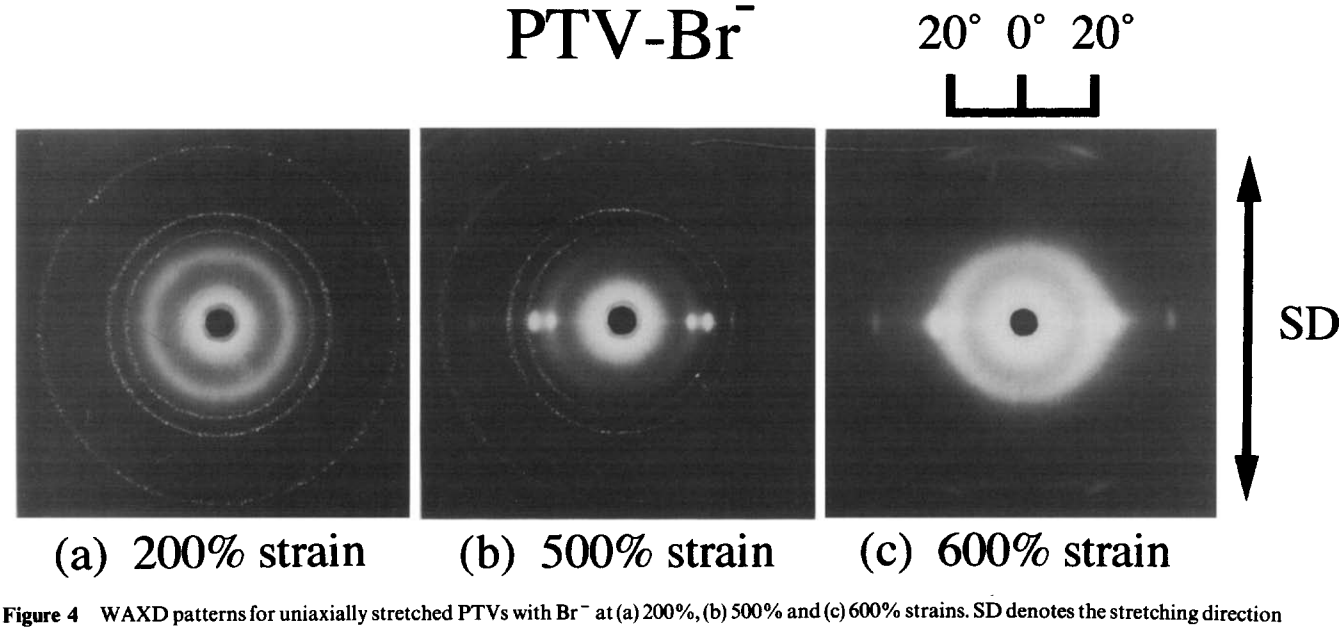

Figure 4 WAXD patterns for uniaxially stretched PTVs with Br^- at (a) 200%, (b) 500% and (c) 600% strains. SD denotes the stretching direction

Table 1 Thermal characteristics[a] of the poly(THF) segments of PTVs measured by d.s.c.

	Counter-anion		
	Cl^-	Br^-	I^-
ΔH_m (cal g^{-1})	13.3	10.3	11.1
T_m (°C)	8.1	6.7	6.2
T_g (°C)	−79.0	−80.6	−83.2
$T_{g,c}$ (°C)	−84.5	−84.6	−84.3
T_c (°C)	−67.8	−65.7	−65.5

[a] T_g, glass transition temperature; T_m, melting temperature; ΔH_m, heat of fusion; $T_{g,c}$, glass transition temperature of the quick quenched samples (see text); T_c, cold crystallization temperature

The thermal characteristics of the poly(THF) segments for the PTVs with Cl^-, Br^-, or I^- counter-anions are listed in *Table 1*, where ΔH_m is the heat of fusion, T_m is the melting temperature (which is approximated by the peak temperature of the endotherm in this study) and T_g is the glass transition temperature. The PTV with Cl^- showed higher ΔH_m than those with Br^- and I^-, and hence had the highest degree of crystallinity of the poly(THF) chains among the three PTVs. The melting temperatures T_m were in the order: $T_m(Cl^-) > T_m(Br^-) \geqslant T_m(I^-)$. Since the higher melting point of crystalline polymers generally implies that the crystallites are more stable on heating, PTV with Cl^- might have the most complete structure of crystallites among the three. Thus, the difference in counter-anions of the viologen hard segments embedded periodically in the PTV backbones affected the degree of crystallinity and the melting temperature of the poly(THF) soft segments. We will consider the effects of the sort of counter-anion on T_m again in relation to the model of microphase-separated structure in *Figure 10*.

The sort of counter-anion also influenced the glass transition temperature T_g of the poly(THF) block; T_g values were in the order: $T_g(Cl^-) > T_g(Br^-) > T_g(I^-)$. The shift in T_g is often discussed in terms of the degree of completion of microphase separation of the hard- and soft-segment blocks in multiphase polymers[15]. According to this interpretation, the PTV with Cl^- has the worst degree of completion of microphase separation among the three specimens. However, this turns out to be incorrect by the SAXS measurements, which are presented in *Figure 8*. The alternative explanation for the shift in T_g is that a constraint on the motion of amorphous poly(THF) chains due to the crystallites of poly(THF) can elevate T_g. Thus, the highest T_g of PTV with Cl^- may come from the highest degree of crystallinity.

In order to confirm the above explanation for the effect of counter-anions on T_g, we performed the following experiment. The PTV with Cl^-, Br^-, or I^- anions was placed in an aluminium pan and the pan was rapidly quenched to −196°C from ambient temperature by dipping it in liquid nitrogen. It was transferred quickly to the furnace of the d.s.c. apparatus prechilled to −180°C, and then the d.s.c. measurements were carried out in the heating process at a rate of 5°C min^{-1}. *Figure 6* depicts the d.s.c. thermograms thus obtained. These rapidly quenched PTVs showed a glass transition temperature ($T_{g,c}$) and a cold crystallization exotherm peak at T_c of the poly(THF) chains, where the latter peaks were not clearly detected in the thermograms in *Figure 5*. As tabulated in *Table 1*, the $T_{g,c}$ values are almost the same irrespective of the sort of counter-anion and are all lower than the values of T_g, the glass transition temperature of the slowly cooled PTV samples (the cooling rate is about 20°C min^{-1}). Therefore, the change in the T_g values for PTVs due to the counter-anions described above is attributed not to the degree of completion of microphase separation between the viologen groups and the poly(THF) chains, but to the degree of constraint on the motion of the amorphous poly(THF) chains due to the poly(THF) crystallites, which are formed in the cooling process prior to successive d.s.c. measurements shown in *Figure 5*.

On the other hand, as shown in *Table 1*, the peak temperatures of the cold crystallization exotherm, T_c, were affected by the counter-anions, and PTV with Cl^- anions exhibited the lowest T_c, indicating that the poly(THF) chains of PTV with Cl^- crystallize most favourably. Therefore, the degree of completion of microphase separation between the soft poly(THF) segments and the hard viologen groups is expected to be higher for PTV having Cl^- anions, which in turn means that the poly(THF) chains are more advantageous to crystallizing than those having Br^- or I^-. We will discuss the effect of the sort of counter-anion on T_c in relation to the model of microphase-separated structures in *Figure 10*.

Dynamic viscoelastic properties

Figure 7 shows the temperature dependence of storage modulus (E') and loss tangent ($\tan\delta$) for PTVs with Cl^-, Br^-, or I^-. The measurements were carried out at a heating rate of 3°C min^{-1}, after the PTV specimens were cooled to −180°C from room temperature at a rate of ca. 15°C min^{-1}. For all PTVs, three peaks around −120, −70 and −5°C are observed in $\tan\delta$ and correspond, respectively, to amorphous relaxation due to the local

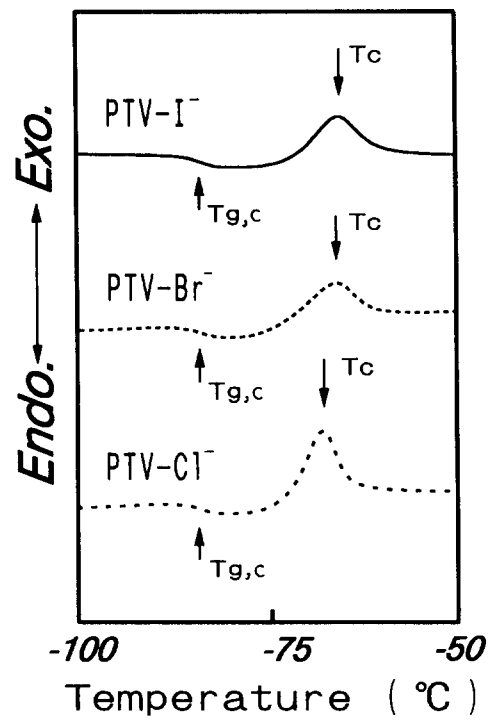

Figure 6 D.s.c. thermograms of PTVs quick quenched to −180°C from room temperature (see text for details): counter-anions as indicated. $T_{g,c}$ and T_c denote the glass transition and cold crystallization temperatures of the poly(THF) chains, respectively

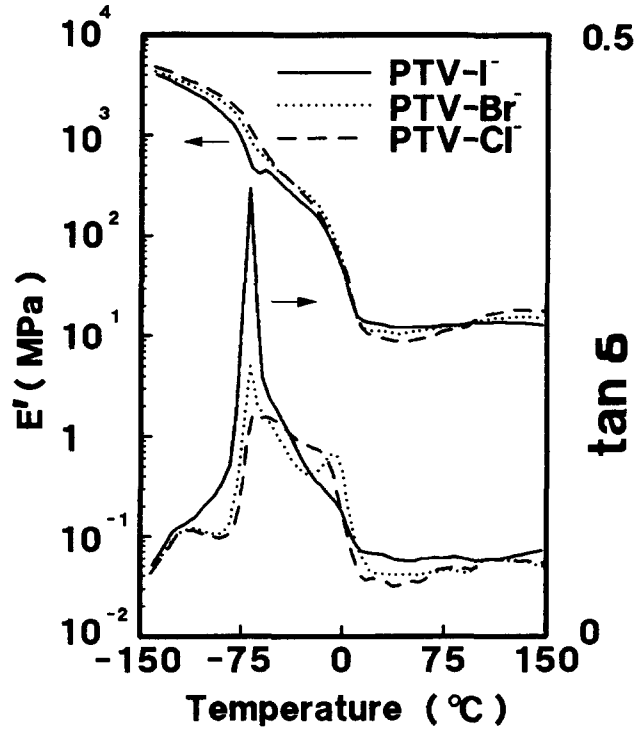

Figure 7 Temperature dependences of storage modulus (E') and loss tangent ($\tan\delta$) for PTVs: counter-anions as indicated

motions of methylene groups[16], to the glass transition of the amorphous poly(THF) chains, and to melting of poly(THF) crystallites formed in the cooling process prior to the dynamic viscoelastic measurements.

The peak heights due to the glass transition of the poly(THF) chains in $\tan\delta$ around -70°C are in the order $PTV(I^-) > PTV(Br^-) > PTV(Cl^-)$, indicating that the quantities of amorphous poly(THF) chains are in this order. The temperatures of the $\tan\delta$ peaks due to the glass transition can be presumably recognized to be in the order $PTV(Cl^-) > PTV(Br^-) \geqslant PTV(I^-)$, which is consistent with the result obtained by the d.s.c. analysis mentioned above. It is noteworthy that the $\tan\delta$ of the PTV with Cl^- shows a very broad peak from -80 to $+5$°C. The ordinary d.s.c. result presented in *Figure 5* exhibited no cold crystallization of the poly(THF) chains for the specimen precooled at a rate of ca. 20°C min^{-1}. Therefore, no contribution due to cold crystallization is taken into account in $\tan\delta$, and hence the broad peak of $\tan\delta$ from -80 to $+5$°C comprises only two contributions. Thus, the $\tan\delta$ peak due to the glass transition of the amorphous poly(THF) can presumably be considered to be broad even after subtracting the contribution due to melting of the poly(THF) crystallites from the original $\tan\delta$ peak. This indicates that the glass transition occurs in a wide temperature range, and therefore a wide distribution is suggested in the degree of constraint on the motion of amorphous poly(THF) chains due to the poly(THF) crystallites. A similar argument may be applied to the PTV with Br^-.

On the other hand, for the PTV with I^-, $\tan\delta$ shows a sharp peak at -70°C. PTV with I^- had fewer poly(THF) crystallites to restrain the motion of the amorphous poly(THF) chains and hence exhibited lower T_g than those with Br^- or Cl^-. In addition, the peak due to melting of the poly(THF) crystallites around -5°C is smaller for PTV with I^- than for those with Br^- or Cl^-.

In the E' vs. temperature curves, all the PTVs showed rubbery plateaux at least until 150°C. This indicates that ionic physical crosslinks are stable even at high temperature, irrespective of the sort of counter-anion.

Feng *et al.*[17] reported that the value of E' increased considerably around 50°C for the same kind of specimen of PTV with $CF_3SO_3^-$ counter-anions, and such a 'jump' in E' might be caused by conformational changes in the ionic hard segments. However, such an E' 'jump' was not clearly observed in the present study for PTVs with Cl^-, Br^-, or I^-.

Thus, the dynamic viscoelastic properties and thermal properties described above show that the counter-anions of the viologen units for PTVs influence the crystallizability of the poly(THF) block chains in the cooling process prior to the dynamic viscoelastic and d.s.c. measurements, and give changes in their mechanical and thermal properties at temperatures below room temperature. The difference in the crystallizability of the poly(THF) chains is attributable to the degree of completion of microphase separation between the soft poly(THF) chains and the hard viologen ionic segments, and the degree of completion of microphase separation is considered to be in the order: $PTV(Cl^-) > PTV(Br^-) \geqslant PTV(I^-)$. In order to confirm this speculation, we conducted SAXS measurements, whose results are shown in the following section.

Microphase-separated structure

Figure 8 shows the logarithm of the Lorentz-corrected scattered intensity, $q^2I(q)$, as a function of the magnitude of the scattering vector, q:

$$q = |\boldsymbol{q}| = (4\pi/\lambda)\sin(\theta/2) \quad (1)$$

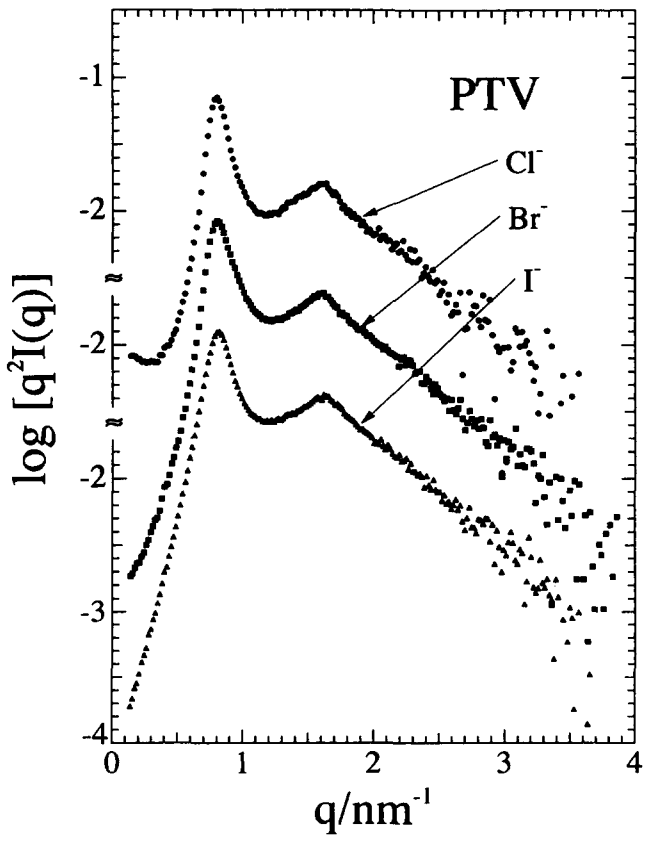

Figure 8 Logarithm of the Lorentz-corrected scattered intensity as a function of the magnitude of the scattering vector, q

where λ and θ are the wavelength of the X-rays ($\lambda = 0.1488$ nm) and the scattering angle, respectively. Since the first- and second-order scattering maxima were observed at their relative q-values closely represented by 1:2 for all specimens, a lamellar microdomain structure can be considered. It is noted that the scattering profiles are almost identical, irrespective of the sort of counter-anion. The first-order maximum is observed at $q = 0.798\ \text{nm}^{-1}$, giving an interdomain distance of 7.87 nm.

Here, it is quite interesting to observe the lamellar microdomain structures in ionomers. Namely, disc-like aggregation of the ionic segments is found by SAXS instead of the spherical aggregation that has been exclusively considered for ionomers[18]. As will be discussed later in *Figure 10*, the lamellar morphology results from the rigid chemical structure of the viologen unit, which is embedded in the polymer chain.

Feng *et al.*[17] reported SAXS profiles for the same kind of PTV specimens with $CF_3SO_3^-$ anions. However, they observed a single and broad scattering peak. They also reported the transmission electron micrograph for the PTV with $CF_3SO_3^-$ anions and observed aggregation that was very different from lamellae. This indicates that the lamellar microdomain structures of the PTVs with Cl^-, Br^-, or I^- anions are more highly ordered than those with $CF_3SO_3^-$ anions, which may be due to stronger ionic attractions for Cl^-, Br^-, or I^- than for $CF_3SO_3^-$. The same research group[19], however, also proposed a lamellar-type morphological model for another poly(THF)-based ionene with Br^- counter-anions, which was prepared from benzyl dibromide and dimethylamino-terminated poly(THF) oligomer.

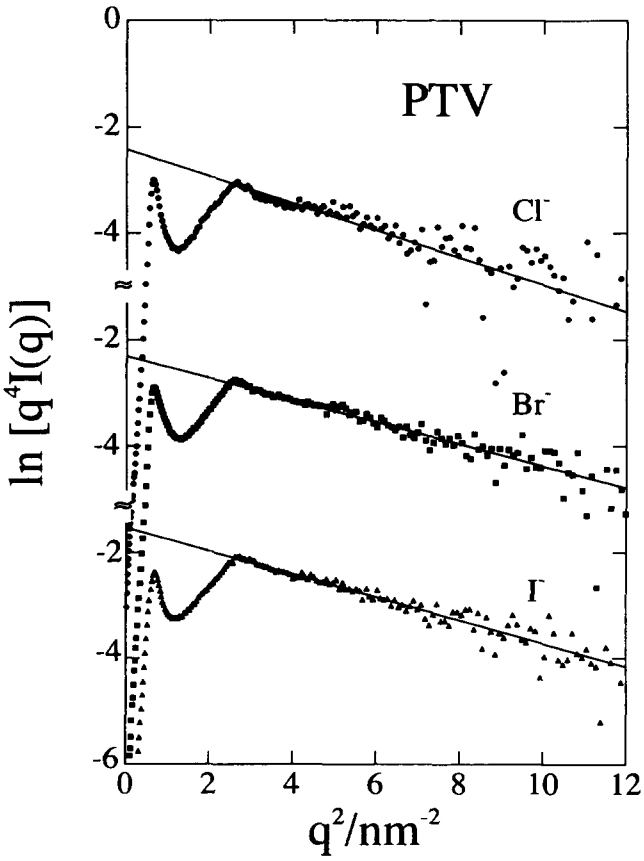

Figure 9 Plots of $\ln[q^4 I(q)]$ vs. q^2 so as to evaluate the interfacial thickness t_1 by means of equations (2) and (3)

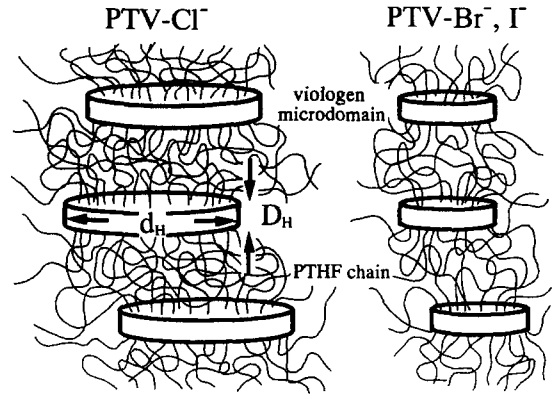

Figure 10 Model for microphase-separated structure for PTVs with Cl^-, Br^-, or I^-. D_H and d_H denote the thickness and the diameter of the disc-like microdomains of the viologen units, respectively. D_H is approximately estimated to be 1 nm

Figure 9 shows the plots of $\ln[q^4 I(q)]$ vs. q^2 so as to evaluate the interfacial thickness t_1 by means of the following equations[20]:

$$I(q) \propto q^{-4} \exp(-\sigma^2 q^2) \qquad \text{for } q \gg 1 \tag{2}$$

with

$$t_1 = \sqrt{2\pi}\,\sigma \tag{3}$$

The parameter σ characterizes the broadness of the interface; for the case of an ideal interface, $\sigma = 0$, which gives Porod's law, i.e. $I(q) \propto q^{-4}$. Least-squares fitting in the region $3 < q^2 < 10$ gives $t_1 = 1.1$–1.2 nm for all specimens.

It is striking to find that SAXS profiles were identical irrespective of the sort of counter-anion, even though the mechanical and thermal properties depended on the sort of counter-anion. In order to explain this, we consider the model for the microphase-separated structure, which is presented in *Figure 10**. It is reasonable to consider that the viologen groups form disc-like microdomains by means of the counter-anions through ionic attraction. The viologen groups may be packed in such a way that their longitudinal directions are parallel to the axis of the disc-like microdomain. The diameter of the disc-like microdomain of the viologen units (d_H) may differ with the attractive force between the viologen units, because d_H is determined by the balance between the ionic attractive force and the elastic force in the lateral direction of the disc resulting from the poly(THF) chains stretched between the viologen microdomains, which will be mentioned in the following paragraph. Since the ionic radius r_i is in the order $r_i(Cl^-) < r_i(Br^-) < r_i(I^-)$, the ionic attractive force should be strongest for Cl^-. Therefore, d_H may be in the order: $d_H(Cl^-) > d_H(Br^-) \geq d_H(I^-)$. The 'grains' of the ordered discs of the viologen microdomains may be spatially randomly oriented in the actual specimen. If the ratio of the free viologen units in the poly(THF) matrix to the total number of viologen units is identical for these PTVs with Cl^-, Br^-, or I^-, i.e. the contrast between hard- and soft-segment microphases is identical for those samples, the difference in d_H hardly affects the SAXS profile. In conclusion, the interdomain distance and its statistical distortion are similar for the PTVs with Cl^-, Br^- and I^-, and therefore the SAXS

* Our literature survey revealed that a similar model of microdomain structure was presented for a telechelic polybutadiene–methacrylic acid copolymer[21]

profiles were identical irrespective of the sort of counter-anion.

We now explore the chain stretching of the poly(THF) block chains. In this discussion, we postulate that the viologen groups of PTVs are exclusively incorporated into the ionic microdomains. The viologen groups are embedded periodically in the PTV backbones and their longitudinal directions are parallel to the axis of the disc-like microdomains as shown in *Figure 10*. Thus, the thickness of the viologen microdomains, D_H, can be identical to the longitudinal length of the viologen group. Thus, D_H is approximately estimated to be 1 nm from its chemical structure. To discuss the chain stretching, the exponent v is estimated using the following equation:

$$D = z^v b + D_H \quad (4)$$

where D, z and b denote the interdomain distance, degree of polymerization of the poly(THF) block chain, and the statistical segment length of poly(THF), respectively. We obtained $v = 0.71$ for all PTVs with Cl^-, Br^-, or I^- using the literature value[15] $b = 0.730$ nm. This analysis quantitatively indicates that the poly(THF) block chains are more stretched than the unperturbed chain ($v = 0.5$). The poly(THF) chains in the vicinity of an interface are forced to be stretched parallel to the longitudinal direction of the viologen units. This is because the distance between the nearest neighbours of the chemical junctions on the interface, which is determined by the packing of the viologen groups, is much smaller than the unperturbed chain dimension. Such a constraint on the chemical junctions may result in chain stretching of the poly(THF) block chains, and in turn may result in the diameter of the viologen disc, d_H, by balancing the elastic force in the lateral direction of the disc due to chain stretching with the ionic attractive force.

The chain stretching in similar ionene polymers with poly(THF) soft segments and benzyl dihalide-based ionic hard segments was recently discussed by Feng and Wilkes[22]. They observed a strong molecular-weight dependence of the interdomain spacing in these polymers and only a slight effect of the sort of counter-anion (Cl^- vs. Br^-) on the interdomain distance. The latter result is apparently consistent with the above-mentioned results for PTVs.

Finally, it should be noted that the model presented in *Figure 10* explains the phenomenological observations of T_m and T_c (*Table 1*) in relation to the sort of counter-anion. For the PTV with Cl^-, the degree of ordering of the amorphous poly(THF) chains is larger than those for PTVs with Br^- or I^- in the vicinity of the interface. Therefore, the poly(THF) chains come to have the largest crystallizability upon cooling for the PTV with Cl^- among the three PTVs, which causes the lowest T_c values. In addition, the poly(THF) crystallites in the PTV with Cl^- have the highest T_m because of the smallest entropic difference on melting, ΔS_m, through the relationship $T_m = \Delta H_m^\circ / \Delta S_m$, where ΔH_m° denotes the heat of fusion of the pure crystallite.

ACKNOWLEDGEMENTS

This work has been performed with the approval of the Photon Factory Program Advisory Committee (Proposal No. 91-218).

REFERENCES

1 Hashimoto, T., Sakurai, S., Morimoto, M., Nomura, S., Kohjiya, S. and Irie, M. 'IUPAC Int. Symp. on New Polymers', Kyoto, November 1991, Preprints, p. 114
2 Kohjiya, S., Hashimoto, T., Yamashita, S. and Irie, M. *Chem. Lett.* 1985, 1497
3 Hashimoto, T., Kohjiya, S., Yamashita, S. and Irie, M. *J. Polym. Sci., Polym. Chem. Edn.* 1991, **29**, 651
4 Kohjiya, S., Hashimoto, T. and Yamashita, S. *J. Appl. Polym. Sci.* 1992, **44**, 555
5 Kohjiya, S., Ohtsuki, T. and Yamashita, S. *Makromol. Chem., Rapid Commun.* 1981, **2**, 417
6 Yamashita, S., Itoi, M., Kohjiya, S. and Kidera, A. *J. Appl. Polym. Sci.* 1988, **35**, 1927
7 Leir, C. M. and Stark, J. E. *J. Appl. Polym. Sci.* 1989, **38**, 1535
8 Kohjiya, S., Ohtsuki, T. and Yamashita, S. 'IUPAC 6th Int. Symp. on Cationic Polymerization and Related Processes', Ghent, Belgium, 1983, Abstract, p. 181
9 Hashimoto, T., Kohjiya, S. and Yamashita, S. *Nippon Gomu Kyokaishi* 1987, **60**(1), 27 (in Japanese)
10 Yamashita, S., Hashimoto, T., Yoshida, T. and Kohjiya, S. *Nippon Gomu Kyokaishi* 1987, **60**(1), 34 (in Japanese)
11 Smith, S. and Hubin, A. *J. Macromol. Sci., Chem. (A)* 1973, **7**, 1399
12 Ueki, T., Hiragi, Y., Kataoka, M., Inoko, Y., Amemiya, Y., Izumi, Y., Tagawa, H. and Muroga, Y. *Biophys. Chem.* 1985, **23**, 115; Tran-Cong, Q., Kawakubo, R. and Sakurai, S. *Polymer* 1994, **35**, 1236; Sakurai, S., Nokuwa, S., Morimoto, M., Shibayama, M. and Nomura, S. *Polymer* in press
13 Imada, K., Miyakawa, T., Chatani, Y., Tadokoro, H. and Murahashi, S. *Makromol. Chem.* 1965, **83**, 113
14 Feng, D., Venkateshwaran, L. N., Wilkes, G. L., Leir, C. M. and Stark, J. E. *J. Appl. Polym. Sci.* 1989, **37**, 1549
15 Shibayama, S., Suetsugu, M., Sakurai, S., Yamamoto, T. and Nomura, S. *Macromolecules* 1991, **24**, 6254
16 Kajiyama, T. and MacKnight, W. J. *Macromolecules* 1969, **2**, 254
17 Feng, D., Wilkes, G. L., Lee, B. and McGrath, J. E. *Polymer* 1992, **33**, 526
18 Register, R. A., Ding, S., Foucart, M., Jerome, R., Hubbard, S. R., Hodgson, K. O. and Cooper, S. L. 'Multiphase Polymers: Blends and Ionomers' (Eds. L. A. Utracki and R. A. Weiss), *ACS Symp. Ser.* **395**, American Chemical Society, Washington, DC, 1989, p. 420 and references therein
19 Feng, D., Wilkes, G. L., Leir, C. M. and Stark, J. E. *J. Macromol. Sci., Chem. (A)* 1989, **26**, 1151
20 Hashimoto, T., Fujimura, M. and Kawai, H. *Macromolecules* 1980, **13**, 1660
21 Moudden. A., Levelut, M. and Pineri, M. *J. Polym. Sci., Polym. Phys. Edn.* 1977, **15**, 1707
22 Feng, D. and Wilkes, G. L. *Macromolecules* 1991, **24**, 6788